



Universiteit
Leiden
The Netherlands

Juvenile Huntington Disease: towards better understanding its unique disease characteristics

Bakels, H.S.

Citation

Bakels, H. S. (2026, February 4). *Juvenile Huntington Disease: towards better understanding its unique disease characteristics*. Retrieved from <https://hdl.handle.net/1887/4289464>

Version: Publisher's Version

[Licence agreement concerning inclusion of doctoral thesis in the Institutional Repository of the University of Leiden](#)

License: <https://hdl.handle.net/1887/4289464>

Note: To cite this publication please use the final published version (if applicable).

CHAPTER 6

GLUT-1 changes in pediatric Huntington Disease brain cortex and fibroblasts: an observational case-control study

Antonella Tramutola, Hannah S Bakels, Federica Perrone, Michela Di Nottia, Tommaso Mazza, Maria Pia Abruzzese, Martina Zoccola, Sara Pagnotta, Rosalba Carrozzo, Susanne T de Bot, Marzia Perluigi, Willeke M C van Roon-Mom, Ferdinando Squitieri

Published as: Tramutola A, Bakels HS, Perrone F, Di Nottia M, Mazza T, Abruzzese MP, Zoccola M, Pagnotta S, Carrozzo R, de Bot ST, Perluigi M, van Roon-Mom WMC, Squitieri F. GLUT-1 changes in paediatric Huntington disease brain cortex and fibroblasts: an observational case-control study. EBioMedicine. 2023 Nov;97:104849.

ABSTRACT

Background: Paediatric Huntington disease with highly expanded mutations (HE-PHD; >80 CAG-repeats) presents atypically, compared to adult-onset Huntington disease (AOHD), with neurodevelopmental delay, epilepsy, abnormal brain glucose metabolism, early striatal damage, and reduced lifespan. Since genetic GLUT-1 deficiency syndrome shows a symptom spectrum similar to HE-PHD, we investigated the potential role of the two main glucose transporters, GLUT-1 and GLUT-3, in HE-PHD.

Methods: We compared GLUT-1 and GLUT-3 protein expression in HE-PHD, juvenile-onset (JOHD), and AOHD brains ($n = 2$; $n = 3$; $n = 6$) and periphery ($n = 3$; $n = 2$; $n = 2$) versus healthy adult controls ($n = 6$; $n = 6$). We also investigated mitochondrial complexes and hexokinase-II protein expression.

Findings: GLUT-1 and GLUT-3 expression were significantly lower in HE-PHD frontal cortex ($p = 0.009$, 95% [CI 13.4, 14.7]; $p = 0.017$, 95% [CI 14.2, 14.5]) versus controls. In fibroblasts, GLUT-1 and GLUT-3 expression were lower compared to controls ($p < 0.0001$, 95% [CI 0.91, 1.09]; $p = 0.046$, 95% [CI 0.93, 1.07]). In the frontal cortex, this occurred without evidence of extensive neuronal degeneration. Patients with HE-PHD had deregulated mitochondrial complex expression, particularly complexes II-III, levels of which were lower in frontal cortex versus controls ($p = 0.027$, 95% [CI 17.1, 17.6]; $p = 0.002$, 95% CI [16.6, 16.9]) and patients with AOHD ($p = 0.052$, 95% [CI 17.0, 17.6]; $p = 0.002$, 95% [CI 16.6, 16.7]). Hexokinase-II expression was also lower in HE-PHD frontal cortex and striatum versus controls ($p = 0.010$, 95% [CI 17.8, 18.2]; $p = 0.045$, 95% [CI 18.6, 18.7]) and in frontal cortex versus patients with AOHD ($p = 0.013$, 95% [CI 17.7, 18.1]). Expression JOHD levels were consistently different to those of HE-PHD but similar to those of AOHD.

Interpretation: Our data suggest a dysfunctional hypometabolic state occurring specifically in paediatric Huntington disease brains.

INTRODUCTION

Huntington Disease (HD) is one of nine autosomal dominant, rare, neurodegenerative, polyglutamine (polyQ) disorders characterised by pathological expansions of a trinucleotide CAG-repeat region encoding polyQ. In HD, the CAG region is located in the HTT gene, which encodes the polyQ region in the huntingtin protein.¹ HD typically manifests between 30 and 40 years of age with a movement disorder (typically chorea), cognitive dysfunction (e.g., abnormal executive functions) and behavioural changes, which are associated with an early progressive neurodegeneration of the cortex and striatum.²

Normal CAG-repeat lengths are usually stably inherited, whereas mutant expansions (>36 repeats) can show instability when transmitted to subsequent generations. A mutant CAG-repeat further increases the risk of somatic CAG expansion and can lead to earlier disease onset, at a juvenile age (i.e., <20 years). Highly expanded (HE) mutations (i.e., >80 CAG-repeats) cause paediatric onset of disease (i.e., during the first decade of life).³

Patients with HE paediatric HD (HE-PHD) often exhibit neurodevelopmental delay or regression and a particularly severe phenotype, resulting in a shorter lifespan when compared to juvenile-onset HD (JOHD), which has relatively shorter CAG-repeat lengths (i.e., <73),³ or adult-onset Huntington disease (AOHD).³ HE-PHD is also associated with a high rate of infantile epilepsy,^{3,4} liver steatosis,⁵ striatal volume loss with preserved brain cortex,^{3,6} and severe striatal glucose hypometabolism.⁷

Abnormal glucose metabolism is a hallmark of several neurodegenerative diseases and is due, at least in part, to altered expression of glucose transporters (GLUTs),⁸ which control glucose uptake into the brain. GLUT-1 and 3 are the major transporters of glucose across the blood-brain barrier and into neurons.⁹

GLUT-1 deficiency syndrome is a rare genetic neurometabolic disorder caused by mutations in the SCL2A1 gene, which results in impaired glucose transport into the brain.¹⁰ Clinically, GLUT-1 deficiency syndrome manifests with neurodevelopmental delay, microcephaly, a high rate of infantile epilepsy, cognitive impairment and varying degrees of spasticity, ataxia, and dystonia¹¹ – a spectrum of symptoms that shares several similarities with HE-PHD.^{3,12,13}

We hypothesised that expression of GLUT-1 and GLUT-3 may underlie HE-PHD pathology and differ from AOHD. We therefore compared GLUT-1 and GLUT-3 expression in the brain and peripheral tissues of patients with HE-PHD, JOHD and AOHD, and control subjects. Furthermore, we postulated that defects in glucose uptake are associated with impaired brain energy metabolism in patients with HD. Thus, we evaluated expression of mitochondrial complexes and hexokinase-II (HK-II) in the brains of the same four populations.

METHODS

Study outcomes

Our primary outcome was to compare protein expression of the main glucose transporters (e.g., GLUT-1, GLUT-3) and associated cargo protein (Rab11-A) in the brain and peripheral tissues of patients with HE-PHD, JOHD and AOHD, and control subjects. Our secondary outcome was to compare protein expression of mitochondrial complexes and HK-II, in the same four cohorts. Additional outcomes included brain and peripheral gene expression of SLC2A1 and SLC2A3, which encode GLUT-1 and GLUT-3 (all four cohorts); GLUT-1 localization in the brain (HE-PHD, AOHD and control cohorts only); and cell counts/neurodegeneration in the brain (HE-PHD cohort only).

Study population and tissue acquisition

HE-PHD was defined as HD manifesting with paediatric onset and a mutant HTT expansion length >80 CAG-repeats,³ a threshold associated with childhood-onset of disease.³ JOHD was defined as HD manifesting with early age of onset, retrospectively indicated in the approximate range of 18–25 years and HTT expansion length >55 CAG-repeats. AOHD was defined as HD manifesting in adulthood at age > 30 years and a mutant HTT expansion length of ≤ 55 CAG-repeats.¹⁴ (Table 1). The CAG-Age Product (CAP) score, considered a predictor of HD progression and a commonly used measure of cumulative exposure to the effects of mutant (CAG expanded) Huntingtin, was calculated for all patients.¹⁵

Table 1. Characteristics of HE-PHD, JHD, AOHD patients and controls involved in fibroblast and brain tissue analyses.

Cohort	Code	Centre	Sex	Tissue	Expanded CAG-repeat ^a	Age of onset (years)	Age/Age of death (years)	CAP at death grade	Vonsattel HD phase	First main symptoms
	HD86 ^b	LUMC	F	FrCx, Striatum	86	4	19	994	3	Final
	HD252	LUMC	F	FrCx, Striatum	83	6	17	839	3	Final
HE-PHD	HD707-02 ^a	LIRH	M	Fibroblasts	114	3.5	5	NA	NA	Initial
	HD130-05 ^{a, b}	LIRH	F	Fibroblasts	95	2	6	NA	NA	Moderate
	HD379-05 ^{a, b}	LIRH	M	Fibroblasts	87	5	7	NA	NA	Moderate
	HD123	LUMC	M	FrCx, Striatum	59	19-22	38	963	2/3	Final
	HD208	LUMC	M	FrCx, Striatum	68	21-23	37	1270	3	Final
JOHD	HD247	LUMC	F	FrCx	56	22-25	44	983	2/3	Final
	HD83-08	LIRH	F	Fibroblasts	56	20-24	35	NA	NA	Advanced
	HD701-01	LIRH	F	Fibroblasts	62	18	30	NA	NA	Advanced
	HD255	LUMC	M	FrCx, Striatum	55	30-33	45	960	3	Final
	HD246	LUMC	M	FrCx, Striatum	44	35	47	486	3	Advanced
	HD234	LUMC	M	FrCx	NK	31	46	NK	3	Final
AOHD	T4161	LIRH	M	FrCx	46	>35	56	691	3	Final
	T1991	LIRH	M	FrCx	48	>35	53	688	3	Cognitive changes
	HD249 ^c	LUMC	F	FrCx, Striatum	46	35	60	740	3	Behavioural changes, chorea
	HD364-06	LIRH	F	Fibroblasts	41	48	50	NA	NA	Initial
	HD598-01	LIRH	M	Fibroblasts	40	54	62	NA	NA	Initial
	E15-02 ^c	LUMC	M	Striatum	NK	NA	54	NA	NA	NA
	E16-07 ^c	LUMC	F	FrCx	18/19	NA	61	NA	NA	NA
	E14-138	LUMC	M	FrCx, Striatum	17/17	NA	48	NA	NA	NA
	T4452	LIRH	M	FrCx	15/20	NA	67	NA	NA	NA
	T4233	LIRH	M	FrCx	16/17	NA	74	NA	NA	NA

Table 1. Continued

Cohort	Code	Centre	Sex	Tissue	Expanded CAG-repeat ^a	Age of onset (years)	Age/Age of death (years)	CAP at Vonsattel death grade	HD phase	First main symptoms
Controls	T4434	URH	F	FCx	18/27	NA	79	NA	NA	NA
	OPBG	F	Fibroblasts	NK	NA	NA	NA	NA	NA	NA
CTR1	OPBG	F	Fibroblasts	NK	NA	NA	NA	NA	NA	NA
CTR2	OPBG	F	Fibroblasts	NK	NA	NA	NA	NA	NA	NA
CTR3	URH	F	Fibroblasts	NK	NA	NA	NA	NA	NA	NA
CTR4	URH	M	Fibroblasts	NK	NA	NA	NA	NA	NA	NA
CTR5	URH	F	Fibroblasts	NK	NA	NA	NA	NA	NA	NA
CTR6	URH	M	Fibroblasts	NK	NA	65	NA	NA	NA	NA

AOHD, adult-onset Huntington disease; CAP, CAG age product; F, female; FCx, frontal cortex; HD, Huntington disease; HE-PHD, highly expanded paediatric Huntington disease; LIRH, Lega Italiana Ricerca Huntington; LUMC, Leiden University Medical Center; JHD, juvenile Huntington disease; M, male; NA, not applicable; NK, not known; OPBG, Ospedale Pediatrico Bambino Gesù.

^aDetailed clinical and genetic description in Graziola et al.¹

^bIndividual with documented epilepsy.

^cSample used for IHC experiments.

Post-mortem brain tissue samples of the frontal cortex and striatum were taken from donor brains of deceased patients with either HE-PHD (n = 2), JOHD (n = 3) or AOHD (n = 6), and healthy adult controls (n = 6) (age-matched to AOHD only, owing to the lack of available donor brains from healthy children) and collected at the Department of Pathology, Leiden University Medical Center (LUMC), Leiden, the Netherlands (Table 1).

Human fibroblast cell lines were generated at the IRCCS Bambino Gesù Children's Hospital (OPBG), Rome, Italy following skin punch biopsies taken from three patients with HE-PHD, two patients with JOHD, two patients with AOHD (all recruited from the Lega Italiana Ricerca Huntington [LIRH] Foundation outpatient clinic) and six age-matched controls (four recruited from the LIRH Foundation and two recruited from the OPBG; Table 1). These patients had also been entered into the ENROLL-HD study, the world's largest observational study for patients with HD and their families, at the LIRH Foundation site.³

Sample size determination

Owing to the rarity of HD, especially HE-PHD, no formal sample size calculations were performed. Indeed, HE-PHD is so rare that its prevalence has yet to be determined. Furthermore, obtaining HE-PHD brain specimens is particularly challenging since it relies on brain donations from deceased children, which is generally considered an exceptional event. Our available sample size of 30 subjects, including patients and healthy controls (brain donors, n = 17; fibroblast donors, n = 13), was therefore based on the number of samples obtainable within a reasonable timeframe for analysis.

Analysis of protein and transcripts

Deep frozen human brain samples and fibroblasts were prepared in radioimmunoprecipitation (RIPA) buffer (50 mM Tris-HCl, 150 mM NaCl, 1% NP-40, 0.25% sodium deoxycholate, 1 mM EDTA, 0.1% SDS, pH 7.4) and phosphatase and protease inhibitors (Sigma-Aldrich). Detailed laboratory procedures for protein expression analysis have been previously described.¹⁶ Briefly, 20 µg of protein preparations from patients and controls were separated via SDS-PAGE using Criterion™ TGX Stain-Free™ precast gels (Bio-Rad Laboratories or ThermoFisher) and transferred to a nitrocellulose or polyvinylidene difluoride membranes by Trans-Blot Turbo Transfer System (Bio-Rad Laboratories). Membranes were probed with the following primary antibodies: GLUT-1 (Ab15309, Abcam, 1:1000, RRID:

AB_301844), GLUT-3 (Ab15311, Abcam, 1:1000, RRID: AB_301846), Rab11-A (sc-166912, Santa Cruz Biotec., 1:1000, RRID: AB_10611645), HK-II (sc-130358, Santa Cruz, 1:1000, RRID: AB_2295219), OXPHOS (Ab110411, Abcam, 1:5000, RRID: AB_2756818), NDUFUB8 (NBP2-75586, NOVUS, 1:5000), and VDAC (PA1-954A, Invitrogen, 1:1000, RRID: AB_2304154). GAPDH (MA5-15738, Invitrogen, 1:1000, RRID: AB_10977387) and anti-Vinculin (V9264, Sigma–Aldrich, 1:1000, RRID: AB_10603627) were the housekeeping proteins used for normalization in brain tissue and fibroblasts, respectively. Immunodetection was performed with horseradish peroxidase (HRP)-conjugated secondary antibodies anti-rabbit (1:10000; L005661, Bio-Rad Laboratories) or anti-mouse (1:10000; L005662, Bio-Rad Laboratories or 1:30000, Jackson Immuno-Research). Blots were then imaged by the ChemiDoc MP imaging system using Chemiluminescence settings. Western blot results were quantified and visualised as percentage of variation relative to controls using Image Lab 6.1 software (Bio-Rad Laboratories). All experiments were performed in triplicate. Total RNA was isolated from patients' and controls' fibroblasts using the Total RNA Purification Plus Kit (Norgen Biotek Corp, Canada) and, for each sample, 2 µg of total RNA was reverse transcribed according to the manufacturer's protocol for M-MLV reverse transcriptase (Promega Italia, Italy). cDNAs were amplified (TaqMan assays) in triplicate with primers for SLC2A1 (Hs00892681_m1), SLC2A3 (Hs00359840_m1), Rab11-A (Hs00366449_g1), Rab11-B (Hs00188448_m1), and GAPDH (Hs99999905_m1) conjugated with fluorochrome FAM (Applied Biosystems Italia). The level of expression was measured by real-time quantitative reverse transcriptase PCR (qRT-PCR) using cycle threshold (Ct). The Ct was obtained by subtracting the Ct value of the gene of interest from the Ct value of the housekeeping gene (GAPDH). Data were analysed using the $2^{-\Delta\Delta Ct}$ method and reported as fold difference relative to controls. The analysis was performed using the QuantStudio™ 12K FlexSoftware v2.2 (Applied Biosystems). All PCR reactions were performed using a QuantStudio 12K Flex Real-Time PCR System (Applied Biosystems).

Immunohistochemistry and cell counts

Formalin-Fixed-Paraffin-Embedded 5 µm brain sections were cut and stained using haematoxylin and eosin (H&E). Immunostaining was performed for GLUT-1 (Ab15309, Abcam, 1:500, RRID: AB_301844) and NeuN (AB104225, Abcam, 1:500, RRID: AB_10711153). Sections were deparaffinised and rehydrated, and subsequent antigen retrieval was performed in citrate buffer (pH 6.0) using a pressure cooker

(15 min). Afterwards, endogenous enzyme block was performed by a 10-min incubation in 3% H_2O_2 in demineralised water, and non-specific antibody block was performed by a 1-h incubation in 1% BSA in PBS-T. Primary antibody incubation was performed overnight (GLUT-1 at room temperature, NeuN at 4 °C), followed by incubation with an anti-rabbit HRP secondary antibody (sc-2030, Santa-Cruz, 1:200) for 1 h at room temperature. Visualization of immunostaining was performed with chromogen 3,30'-diaminobenzidine (DAB). Finally, sections were counterstained with haematoxylin, dehydrated and cover slipped. The slides were digitised using an automatic bright field microscope (Philips Ultra Fast Scanner, Philips, Netherlands) for microscopic evaluation and taking pictures. For easy visualization purposes of GLUT-1 immunopositivity, a binary mask of the DAB signal was established by use of free Image-J software (colour deconvolution, grey scale 8-bit, threshold grey value 0–188, binary mask).

The total number of neurons in HE-PHD donors was estimated by stereological analyses of NeuN-stained slides by use of free QuPath software (positive cell detection, optical density sum, cell intensity threshold: DAB OD max) (Supplementary Fig. S1). Per slide, the mean number of neurons per mm^2 was calculated in three separate areas by analyzing cortical layers I to VI. Cell counts were performed by a single individual (HSB).

Fibroblast cell lines

Human cultured fibroblasts were obtained from skin biopsy of patients and aged matched controls. Human fibroblasts were cultured in Dulbecco's Modified Eagle Medium high glucose (4.5 g/l) supplemented with 10% foetal bovine serum, 50 $\mu\text{g}/\text{ml}$ uridine and 110 mg/l sodium pyruvate. To analyse cell cycle status, 5×10^5 fibroblasts from patients and controls were plated and harvested at about 80% confluence. 2×10^6 cells were washed with PBS and centrifuged for 5 min at 1500 rpm at 4 °C. The obtained pellet was fixed with a cold solution of methanol/acetone 2:1 (v/v) by gently vortexing, and incubated over night at 4 °C. The next day, cells were centrifuged at 1100 rpm for 5 min at 4 °C and the pellet was re-suspended in a solution containing propidium iodide 500 $\mu\text{g}/\text{ml}$ and RNase 1 mg/ml and incubated for 30 min at room temperature. After incubation, cells were analysed by flow cytometry (BD LSRII Fortessa X-20, BD Biosciences).

Statistics

Patient data were expressed as mean \pm standard error of the mean (SEM). For brain tissue, densitometry data were first log-transformed and then analysed using Analysis of Variance (ANOVA) to assess the overall differences among groups, i.e., controls, HE-PHD, JOHD, and AOHD. Subsequently, post-hoc comparisons were conducted using the Tukey multiple comparisons of means test or the Wilcoxon rank sum exact test, in case of deviation from normality. Normality was assessed using the Shapiro–Wilk normality test. Multiplicity was not considered in this study. All statistical tests were two-tailed, and the level of significance was set at $p < 0.05$. Statistical analyses were performed using the R software (version 4.2.2, R Foundation for Statistical Computing, Vienna, Austria).

Ethics

Samples were provided to the LIRH Foundation for research purposes. This study was performed in accordance with the ethical principles outlined in the World Medical Association Declaration of Helsinki. Pseudo-anonymization of all donors was preserved by using a coded system for the tissue samples. Clinical study protocols and informed consent forms for patients and healthy controls were approved by the Institutional Review Board of the LIRH Foundation on 28th October 2022 (n. 10.281022).

Role of the funding source

The funding source had no role in study design, data collection and interpretation, analysis, writing of this report, or in the decision to submit the paper for publication.

RESULTS

Study population and tissue acquisition

In total, 17 deceased donors were identified for the brain tissue analyses (HE-PHD, $n = 2$; JOHD, $n = 3$; AOHD, $n = 6$; healthy adult controls, $n = 6$) and 13 individuals participated in the fibroblast analyses (HE-PHD, $n = 3$; JOHD, $n = 2$; AOHD, $n = 2$; healthy adult controls, $n = 6$) (Fig. 1; Table 1).

All patients in the HE-PHD cohort ($n = 5$) showed childhood onset of disease at <10 years of age (Table 1). The HTT mutation was inherited maternally in one patient and transmitted paternally in all other patients.

Post-mortem delay (<12 h) was comparable between controls, patients with HE-PHD, JOHD and AOHD. All striatal samples from patients with HD were categorised as Vonsattel neuropathological grade 3 (Table 1). Further clinical and neuropathological characteristics of the HE-PHD brain donors are also included in Table 1.

Patients of any sex were eligible for inclusion in this study. Sex was self-reported by participants or, for deceased donors, documented per the patient's medical records.

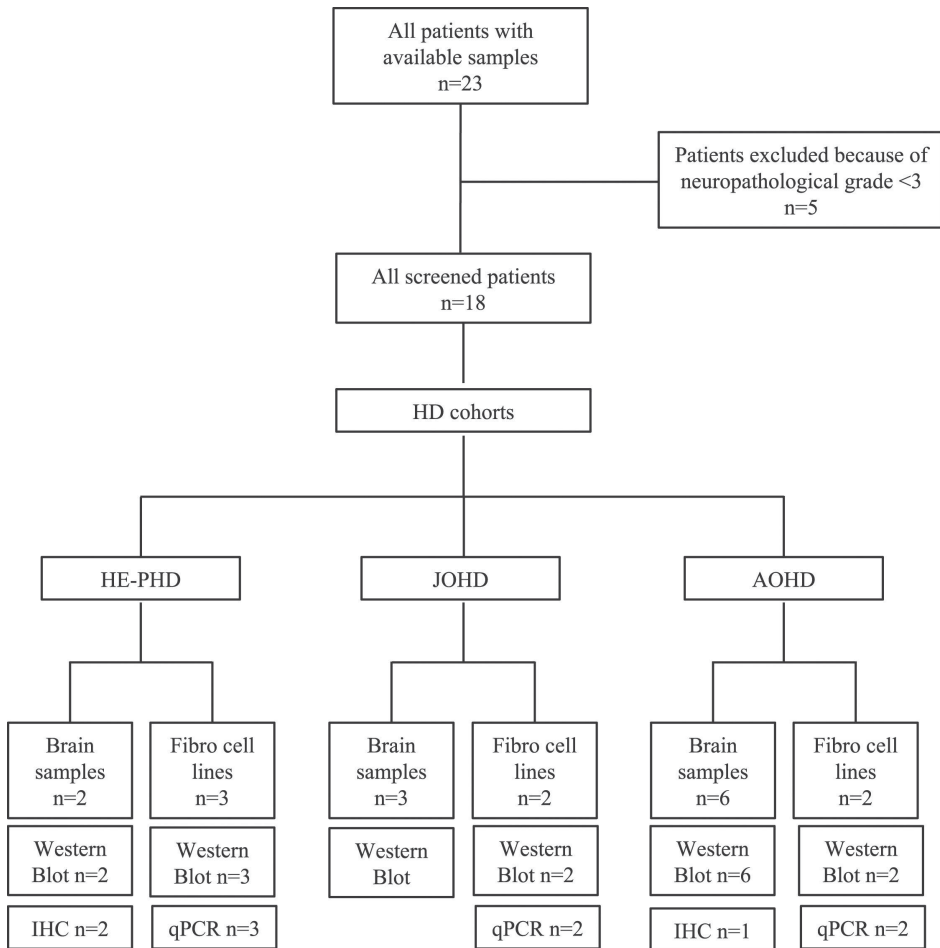


Figure 1. Study design, participants, and procedures. IHC = immunohistochemistry.

Low GLUT-1 expression in HE-PHD tissues

The ANOVA test for GLUT-1 protein expression revealed a statistically significant difference among groups in the frontal cortex ($F (3, 10) = 5.93, p = 0.014$), but not in the striatum ($F (3, 4) = 3.054, p = 0.15$). In the frontal cortex of donors with HE-PHD, the GLUT-1 protein expression level was ~4 or 5 times lower than in the JOHD, AOHD, or control samples (Fig. 2a and b; Table 2). The protein expression level of GLUT-1 was also lower in the striatum of donors with HE-PHD than in all other groups, although this difference was not statistically significant (Fig. 2c and d; Table 2). In contrast, neither JOHD nor AOHD samples showed any significant difference in GLUT-1 expression in the frontal cortex or in the striatum when compared to the control samples (Tukey test, frontal cortex: JOHD $p = 0.884$, 95% CI $[-1.25, 0.77]$, AOHD $p = 0.704$, 95% CI $[1.21, -0.57]$; striatum: JOHD $p = 0.407$, 95% CI $[-5.81, 2.35]$, AOHD $p = 0.698$, 95% CI $[-2.99, 5.17]$) (Fig. 2a–d). The expression levels of GLUT-1 protein and SLC2A1 mRNA were 2 to ~7 times statistically significantly lower in peripheral fibroblasts of donors with HE-PHD than in all other groups (Fig. 2e–i; Table 3). On the other hand, GLUT-1 protein and SLC2A1 mRNA levels were statistically significantly greater in peripheral fibroblasts of donors with JOHD (Wilcoxon rank sum exact test, protein $W = 132, p = 0.0002$, 95% CI $[0.65, 2.35]$; mRNA $W = 126, p = 0.0003$, 95% CI $[1.23, 1.77]$) and AOHD (Wilcoxon rank sum exact test, protein $W = 123, p = 0.0016$, 95% CI $[0.17, 0.62]$; mRNA $W = 100, p = 0.0332$, 95% CI $[0.05, 2.49]$) than in controls (Fig. 2e–i).

GLUT-1 localization was predominantly found in endothelial cells lining parenchymal capillaries of HE-PHD, AOHD and control brain tissues. In the frontal cortex of HE-PHD donors, a patchy lack of GLUT-1 immunopositivity and reduced expression was observed, as compared to the adjacent subcortical white matter within the same donor (Fig. 2j). Also, in the frontal cortex, a smaller length and less branching complexity of capillaries was visualized in donors with HE-PHD, as compared to donors with AOHD and control (Fig. 2j). GLUT-1 visualization in the caudal neostriatum of HE-PHD donors revealed areas with low or no immunopositivity, as compared to the adjacent capsular white matter showing a regular signal (Fig. 2j). In addition, the length and branching complexity of GLUT-1 positive capillaries in the striatum appeared lower as compared to donors with AOHD and control (Fig. 2j).

Limited neurodegeneration in the frontal cortex of patients with HE-PHD

Microscopic analysis of the frontal cortex revealed limited signs of degeneration (i.e., eccentric nucleus and eosinophilic cytoplasm) and neuronal loss in one donor

with HE-PHD (HD86; mean neuronal cell count, 349 per mm²), and normal structure and architecture of the neocortex in the other (HD252; mean neuronal cell count 493 per mm²) (Supplementary Fig. S2a and b). Conversely, in both patients there was remarkable neuronal loss in the striatum, in line with Vonsattel grade 3.

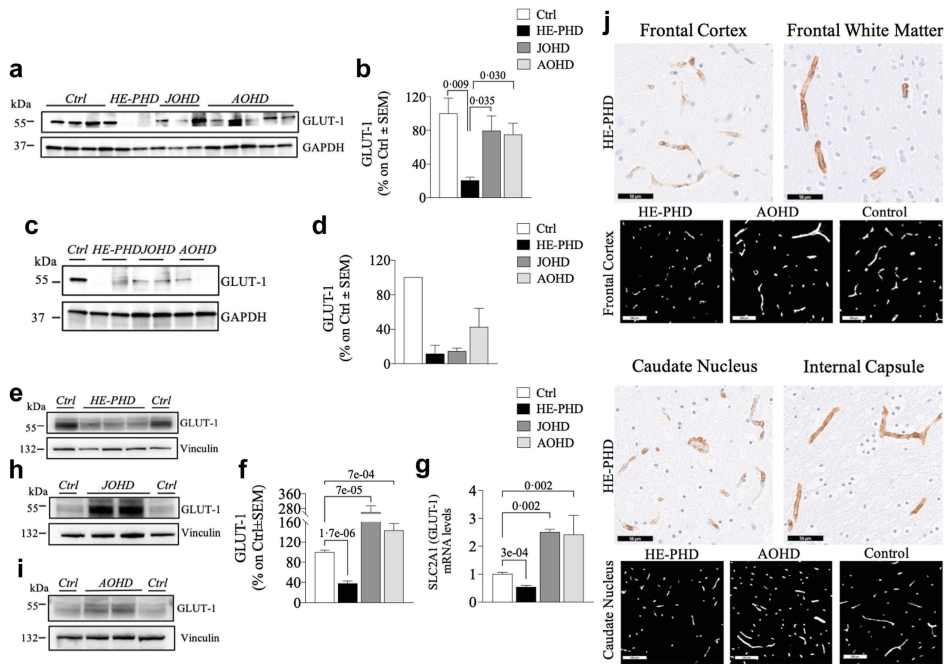


Figure 2. GLUT-1 in brain tissues and fibroblasts of patients with HE-PHD, JOHD and AOHD and controls.

Representative Western blot images and densitometric evaluation of GLUT-1 protein levels normalised to GAPDH or Vinculin protein levels in the FrCx (a, b) striatum (c, d) and fibroblasts (e, f, h, i) of patients with HE-PHD, JOHD and AOHD and healthy adult controls. All densitometric values are reported as a percentage of controls (set at 100%) and are the mean \pm SEM of three independent experiments ($p < 0.05$, one-way ANOVA with Tukey multiple comparisons of means or Wilcoxon rank sum exact post-hoc tests). qRT-PCR analysis of SLC2A1 (GLUT-1) total mRNA in fibroblasts of patients with HE-PHD, JOHD and AOHD and controls (g). Relative mRNA levels were normalised using GAPDH and were calculated as $2^{-\Delta Ct}$. Results are the mean \pm SEM of three independent experiments ($p < 0.05$, one-way ANOVA with Tukey multiple comparisons of means post-hoc test). IHC staining of GLUT-1 in the FrCx (white matter) of HE-PHD donor HD252 (j). Smaller length and lower branching complexity of immune-positive capillaries in the FrCx of HE-PHD donor HD252, as compared to AOHD donor HD249 and healthy control donor E16-07. Scale bars: 100 μ m. GLUT-1 IHC staining in the striatum (caudate nucleus, internal capsule) of HE-PHD donor (HD86) (j). Binary representation of the DAB signal, illustrating smaller length and lower branching complexity of immune-positive capillaries in the caudate nucleus of HD86, as compared to AOHD donor HD249 and healthy control donor E15-02. Scale bars 50 μ m. The use of the same loading control in different figures serves as a representative image. Each individual protein has been normalized against its respective loading control.

Table 2.

Protein	Cohort	Frontal cortex	Striatum
GLUT1	HE-PHD	12.5 ± 0.19 (10.1, 14.9)	9.83 ± 1.30 (-6.67, 26.3)
	Ctrl	14.0 ± 0.19 (13.4, 14.7) [p = 0.009]	12.8 ± 0.12 (11.2, 14.4) [p = 0.129]
	JOHD	13.8 ± 0.27 (12.7, 15.0) [p = 0.035]	11.0 ± 0.07 (10.1, 12.0) [p = 0.65]
	AOHD	13.7 ± 0.21 (13.1, 14.3) [p = 0.030]	11.7 ± 0.56 (4.57, 18.8) [p = 0.376]
GLUT3	HE-PHD	13.1 ± 0.44 (7.50, 18.7)	13.3 ± 0.20 (10.7, 15.9)
	Ctrl	14.3 ± 0.05 (14.2, 14.5) [p = 0.017]	14.5 ± 0.02 (14.3, 14.7) [p = 0.022]
	JOHD	13.0 ± 0.70 (10.0, 16.1) [p = 0.987]	13.3 ± 0.21 (10.7, 16.0) [p = 0.999]
	AOHD	13.7 ± 0.21 (13.2, 14.3) [p = 0.440]	13.8 ± 0.15 (11.9, 15.7) [p = 0.309]
Rab11-A	HE-PHD	16.3 ± 0.02 (16.1, 16.5)	16.5 ± 0.49 (10.3, 22.7)
	Ctrl	17.4 ± 0.08 (17.1, 17.6) [p = 0.011]	17.6 ± 0.01 (17.6, 17.6) [p = 0.170]
	JOHD	16.9 ± 0.34 (15.5, 18.4) [p = 0.175]	17.3 ± 0.31 (13.3, 21.3) [p = 0.377]
	AOHD	17.4 ± 0.09 (17.1, 17.6) [p = 0.010]	17.3 ± 0.12 (15.8, 18.7) [p = 0.404]
HK-II	HE-PHD	16.7 ± 0.21 (14.0, 19.4)	16.7 ± 0.59 (9.2, 24.2)
	Ctrl	18.0 ± 0.12 (17.8, 18.2) [p = 0.010]	18.6 ± 0.01 (18.6, 18.7) [p = 0.045]
	JOHD	17.5 ± 0.44 (15.6, 19.4) [p = 0.131]	17.7 ± 0.22 (14.8, 20.5) [p = 0.283]
	AOHD	17.9 ± 0.06 (17.7, 18.1) [p = 0.013]	17.9 ± 0.14 (16.0, 19.7) [p = 0.193]
Complex I	HE-PHD	16.9 ± 0.62 (9.0, 24.8)	18.1 ± 0.11 (17.4, 20.1)
	Ctrl	17.6 ± 0.19 (17.0, 18.3) [p = 0.155]	18.7 ± 0.01 (18.7, 18.8) [p = 0.230]
	JOHD	17.9 ± 0.21 (17.4, 18.5) [p = 0.049]	18.4 ± 0.03 (18.0, 18.9) [p = 0.633]
	AOHD	17.8 ± 0.06 (17.6, 18.0) [p = 0.064]	18.8 ± 0.11 (17.4, 20.1) [p = 0.173]
Complex II	HE-PHD	16.7 ± 0.15 (14.8, 18.6)	15.8 ± 0.19 (13.3, 18.2)
	Ctrl	17.4 ± 0.09 (17.1, 17.6) [p = 0.027]	17.3 ± 0.01 (17.3, 17.4) [p = 0.024]
	JOHD	17.2 ± 0.13 (16.6, 17.7) [p = 0.150]	17.0 ± 0.33 (12.8, 21.2) [p = 0.048]
	AOHD	17.3 ± 0.11 (17.0, 17.6) [p = 0.052]	16.7 ± 0.19 (14.3, 19.2) [p = 0.099]
Complex III	HE-PHD	15.6 ± 0.41 (10.3, 20.8)	17.6 ± 0.43 (12.1, 23.1)
	Ctrl	16.7 ± 0.05 (16.6, 16.9) [p = 0.002]	19.1 ± 0.01 (19.1, 19.2) [p = 0.029]
	JOHD	16.1 ± 0.21 (15.2, 17.0) [p = 0.061]	18.4 ± 0.03 (17.9, 18.8) [p = 0.215]
	AOHD	16.6 ± 0.01 (16.6, 16.7) [p = 0.002]	18.3 ± 0.03 (18.0, 18.7) [p = 0.246]
Complex IV	HE-PHD	16.0 ± 0.75 (6.48, 25.6)	16.2 ± 0.51 (9.76, 22.6)
	Ctrl	17.6 ± 0.11 (17.2, 17.9) [p = 0.217]	18.9 ± 0.01 (18.9, 19.1) [p = 0.010]
	JOHD	17.1 ± 0.94 (13.1, 21.2) [p = 0.501]	17.5 ± 0.15 (15.6, 19.3) [p = 0.120]
	AOHD	17.8 ± 0.13 (17.4, 18.1) [p = 0.123]	17.8 ± 0.28 (14.3, 21.4) [p = 0.058]
Complex V	HE-PHD	15.7 ± 0.14 (13.9, 17.5)	16.8 ± 0.31 (12.8, 20.8)
	Ctrl	16.2 ± 0.13 (15.8, 16.6) [p = 0.161]	18.2 ± 0.02 (18.2, 28.5) [p = 0.012]
	JOHD	16.2 ± 0.21 (15.3, 17.0) [p = 0.246]	17.4 ± 0.02 (17.2, 17.6) [p = 0.172]
	AOHD	16.2 ± 0.14 (13.9, 17.5) [p = 0.156]	17.3 ± 0.07 (16.3, 18.2) [p = 0.277]

Assessment of highly expanded (HE) Paediatric Huntington disease (PHD) compared with control (Ctrl), juvenile-onset (JOHD), and Adult-Onset HD (AOHD) individuals. Summary of average log-transformed protein expression levels ± SEM, Confidence Intervals (lower, upper), and [p-values] in the frontal cortex and striatum of highly expanded paediatric (HE-PHD) compared to juvenile-onset HD (JOHD), adult-onset HD (AOHD) and control (Ctrl) individuals.

Table 3.

Protein	Cohort	Levels
GLUT1	HE-PHD	0.38 ± 0.17 (0.27, 0.48)
	Ctrl	1.00 ± 0.04 (0.91, 1.09) [p = 1.7e-06]
	JOHD	2.59 ± 0.35 (1.68, 3.49) [p = 7e-05]
	AOHD	1.43 ± 0.14 (1.08, 1.79) [p = 7e-04]
Gene exp.		
SLC2A1	HE-PHD	0.54 ± 0.05 (0.41, 0.67)
	Ctrl	1.02 ± 0.08 (0.83, 1.21) [p = 3e-04]
	JOHD	2.51 ± 0.09 (2.25, 2.76) [p = 0.002]
	AOHD	2.43 ± 0.69 (0.65, 4.20) [p = 0.002]
Protein		
GLUT3	HE-PHD	0.87 ± 0.04 (0.79, 0.97)
	Ctrl	1.05 ± 0.03 (0.93, 1.07) [p = 0.046]
	JOHD	1.09 ± 0.09 (0.99, 1.20) [p = 0.002]
	AOHD	1.12 ± 0.09 (0.89, 1.34) [p = 0.045]
Gene exp.		
SLC2A3	HE-PHD	0.89 ± 0.12 (0.61, 1.19)
	Ctrl	1.11 ± 0.18 (0.67, 1.55) [p = 0.359]
	JOHD	1.18 ± 0.17 (0.75, 1.62) [p = 0.204]
	AOHD	1.70 ± 0.58 (0.19, 3.20) [p = 0.573]
Protein		
Rab11-A	HE-PHD	1.06 ± 0.06 (0.93, 1.19)
	Ctrl	1.00 ± 0.05 (0.89, 1.11) [p = 0.434]
	JOHD	1.14 ± 0.09 (1.04, 1.23) [p = 0.840]
	AOHD	1.06 ± 0.08 (0.85, 1.26) [p = 1]
Gene exp.		
Rab11-A	HE-PHD	0.93 ± 0.08 (0.73, 1.13)
	Ctrl	1.00 ± 0.32 (0.92, 1.08) [p = 0.443]
	JOHD	0.87 ± 0.06 (0.71, 1.02) [p = 0.569]
	AOHD	1.66 ± 0.52 (0.33, 2.99) [p = 0.175]

Assessment of highly expanded (HE) Paediatric Huntington disease (PHD) compared with control (Ctrl), juvenile-onset (JOHD), and Adult-Onset HD (AOHD) individuals. Summary of average protein and gene expression levels ± SEM, Confidence Intervals (lower, upper), and [p-values] in fibroblast cell lines of highly expanded paediatric (HE-PHD) compared to juvenile-onset HD (JOHD), adult-onset HD (AOHD) and control (Ctrl) individuals.

Low GLUT-3 and Rab11-A expression in HE-PHD tissues

The protein expression levels of GLUT-3 were globally significantly different among groups, both in the frontal cortex (ANOVA test, $F (3, 10) = 7.05, p = 0.0079$) and in the striatum (ANOVA test, $F (3, 4) = 11.6, p = 0.019$). Compared to controls, protein

expression levels of GLUT-3 were significantly lower in both the frontal cortex and striatum of donors with HE-PHD (Fig. 3a–d; Table 2). GLUT-3 was also lower in donors with AOHD compared to controls in the frontal cortex (Tukey test, $p = 0.066$, 95% CI [−1.28, 0.14]) (Fig. 3a–d), and lower in donors with JOHD compared to controls in both the frontal cortex (Tukey test, $p = 0.014$, 95% CI [−6.26, −5.32]) and striatum (Tukey test, $p = 0.025$, 95% CI [−2.09, −0.21]). In peripheral fibroblasts, *SLC2A3* gene expression was not statistically significantly different between any group (Table 3), whereas its protein expression was statistically significantly lower in donors with HE-PHD when compared to donors with JOHD, AOHD and controls (Supplementary Fig. S1a–e; Table 3).

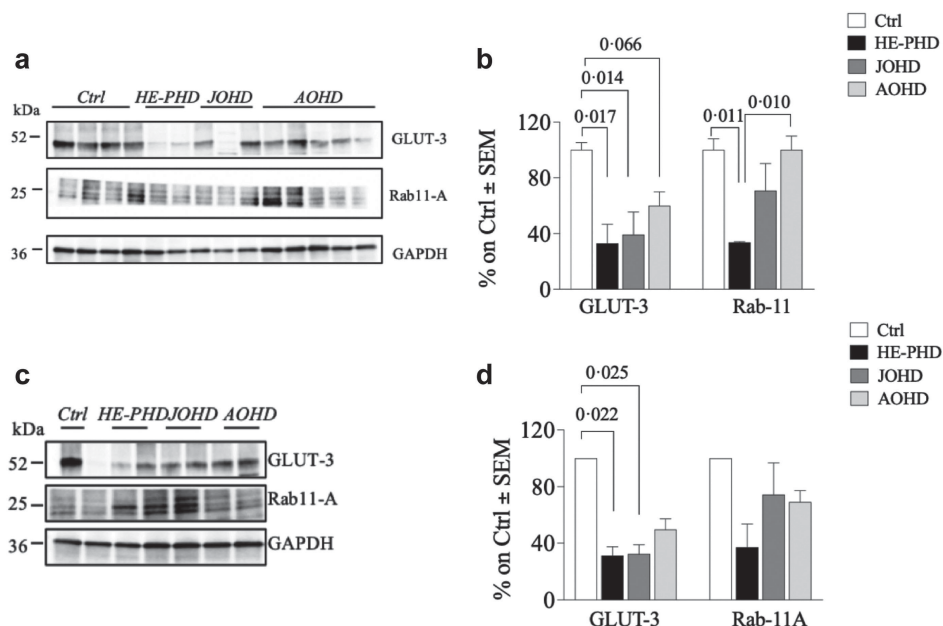


Figure 3. Evaluation of GLUT-3 and Rab11-A levels in brain tissues of patients with HE-PHD, JOHD, AOHD and controls.

Representative Western blot images and densitometric evaluation of GLUT-3 and Rab11-A protein levels normalised to GAPDH protein levels in the FrCx (a, b) and striatum (c, d) of patients with HE-PHD, JOHD and AOHD and healthy adult controls. All densitometric values are reported as a percentage of controls (set at 100%) and are the mean \pm SEM of three experiments ($p < 0.05$, one-way ANOVA with Tukey multiple comparisons of means post-hoc test). The use of the same loading control in different figures serves as a representative image. Each individual protein has been normalized against its respective loading control.

Expression levels of the cargo protein Rab11-A were significantly lower in the frontal cortex of donors with HE-PHD compared to both controls (Tukey test, $p = 0.011$,

95% CI [-1.91, -0.25]) and AOHD (Tukey test, $p = 0.010$, 95% CI [-1.87, -0.27]) (Fig. 3a and b). Data collected in the striatum did not show any differences in Rab11-A protein levels between the HE-PHD cohort and any other cohort (Fig. 3c and d). Rab11-A protein levels in fibroblasts also did not differ between the HE-PHD cohort and any other cohort (Supplementary Fig. S1a, d–g; Table 3).

Impairment in glucose uptake is associated with defects of mitochondrial machinery in patients with HE-PHD

Mitochondrial complex expression was dysregulated in the brains of patients with HD. In particular, levels of complex II and complex III subunits were significantly lower in the frontal cortex of donors with HE-PHD, compared to controls (Tukey test, $p = 0.027$, 95% CI [-1.22, -0.074] and $p = 0.002$, 95% CI [-1.82, -0.48], respectively) and compared to patients with AOHD (Tukey test, $p = 0.052$, 95% CI [-1.09, 0.005], and $p = 0.002$, 95% CI [-1.73, -0.43], respectively) (Fig. 4a, c; Table 2). Furthermore, the expression level of the complex I subunit in HE-PHD was statistically significantly lower compared to donors with JOHD (Tukey test, $p = 0.049$, 95% CI [-2.10, -0.006]), and numerically lower compared to donors with AOHD, following a trend towards statistical significance (Tukey test, $p = 0.064$, 95% CI [-1.87, 0.048]) (Fig. 4a, c; Table 2). We also evaluated levels of complex IV and V (ATP synthase) and voltage-dependent anion-selective channel, a protein that plays a key role in maintaining high rates of oxidative phosphorylation.¹⁷ No statistically significant differences between groups were observed for either protein in the frontal cortex.

Deregulation of mitochondrial complexes expression was also observed in the striatum, with statistically significantly lower levels of all complexes, except complex I, seen in patients with HE-PHD compared to controls (Fig. 4d, f; Table 2).

The HE-PHD cohort showed statistically significantly lower levels of HK-II protein expression in the frontal cortex and striatum, compared to controls (Tukey test, $p = 0.010$, 95% CI [-2.30, -0.33], and $p = 0.045$, 95% CI [-3.78, -0.06], respectively) and in the frontal cortex compared to AOHD (Tukey test, $p = 0.013$, 95% CI [-2.18, -0.27]) (Fig. 4a, b, d, e; Table 2). In contrast, no difference in HK-II protein expression in the frontal cortex was observed between the AOHD and control cohorts (Tukey test, $p = 0.982$, 95% CI [0.86, -0.67]; striatum, $p = 0.443$, 95% CI [2.62, -1.10]). In peripheral fibroblasts, HK-II protein expression differed only between the JOHD and control cohorts (Tukey test, $p = 0.014$, 95% CI [0.07, 0.77]) (Supplementary Fig. S1h–k).

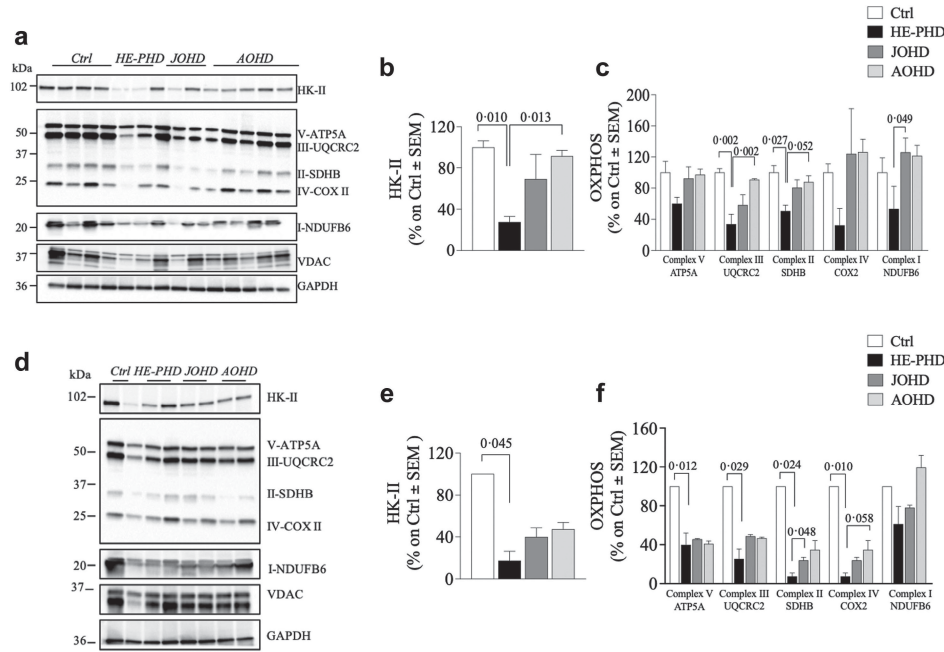


Figure 4. Evaluation of HK-II and mitochondrial machinery complexes (OXPHOS) levels in brain tissues of patients with HE-PHD, JOHD, AOHD and controls.

Representative Western blot images and densitometric evaluation of HK-II and OXPHOS protein levels normalised to GAPDH protein levels in the FrCx (a-c) and striatum (d-f) of patients with HE-PHD, JOHD and AOHD and healthy adult controls. All densitometric values are reported as a percentage of controls (set at 100%) and are presented as the mean \pm SEM of three independent experiments ($p < 0.05$, one-way ANOVA with Tukey multiple comparisons of means post-hoc test). The use of the same loading control in different figures serves as a representative image. Each individual protein has been normalized against its respective loading control.

DISCUSSION

Neurodegenerative conditions, such as Alzheimer, Huntington, and Parkinson diseases, are associated with brain glucose hypometabolism, which is contributed to by impaired GLUT-1 and GLUT-3 glucose transporters.⁸ Interestingly, dysregulation in GLUT transporters has also been observed in aberrant brain neurodevelopment,¹⁸ micromalformations¹⁹ and epilepsy, all conditions that have been associated with HD.^{3,4,20,21}

Patients with HE-PHD manifest signs and symptoms that are uncommon to AOHD, including high frequency of epileptic seizures, early onset hypokinetic-rigid syndrome/dystonia and developmental delay.^{3,4} Interestingly, certain HE-PHD clinical features,

such as epilepsy, are also observed in patients with GLUT-1 deficiency syndrome, where genetic defects in this transporter result in a chronic shortage of glucose in the brain.²² This suggests that alterations in glucose transport or metabolism may also occur in HE-PHD and could explain some of its unique symptoms, compared to AOHD.

In the context of HD, this study demonstrates reduced protein expression of GLUT-1 and GLUT-3 in the frontal cortex and striatum of brains from patients with HE-PHD, compared to brains from patients affected since adulthood, including JOHD, and from controls. Our results are partly in line with others, who have reported significantly lower GLUT-1 and GLUT-3 protein expression in the striatum of late-stage AOHD (classified as neuropathological Vonsattel grade 3), compared to earlier-stage AOHD (neuropathological Vonsattel grades 1 and 2).²⁰ However, they found no evidence of reduced GLUT-1 and GLUT-3 expression in AOHD cortex,²³ whereas in our frontal cortex samples we found statistically significantly lower GLUT-1 expression in patients with HE-PHD versus controls, and statistically significantly lower GLUT-3 expression in all cohorts (HE-PHD, JOHD and AOHD) versus controls.

Furthermore, we identified reduced protein levels of Rab11-A in HE-PHD frontal cortex. Rab11-A is a small GTPase that has a critical role in regulating the trafficking of GLUT-3 to the neuronal cell surface,²⁴ experiments in HD cell models have shown reduced neuronal GLUT-3²⁵ and Rab11-A expression levels and highlights the relevance of altered glucose transportation in models with HE mutations.

In HE-PHD brain samples, low levels of GLUT-1 and GLUT-3 were observed alongside low levels of mitochondrial complexes involved in energy metabolism. In the frontal cortex, significant differences versus controls and versus AOHD were seen for complexes II and III and versus JOHD for complex I. Results from in vitro studies have revealed calcium abnormalities in mitochondria from patients and transgenic mice with HD, and that these defects are a direct effect of HE polyQ.²⁶ Our findings in brain tissues affected by HE HTT mutations, therefore, corroborate these in vitro observations.

Furthermore, we also observed significantly lower levels of HK-II in HE-PHD but not AOHD brains compared to control. Hexokinases catalyse the first committed step of glucose metabolism, by phosphorylating glucose to glucose-6-phosphate.²⁷ HK-II also protects cells from death during hypoxia and functions as a sensor of glucose availability, inducing apoptosis in response to glucose depletion.²⁸

Our finding, that expression levels of GLUT-1, GLUT-3, mitochondrial complexes and HK-II were significantly and selectively lower in HE-PHD frontal cortex and striatum, shows that a disease-relevant biological dysfunction (i.e., hypometabolic state) occurs without any substantial neuronal loss in the frontal cortex of these patients. Relatively preserved brain cortex has been observed previously in HE-PHD by magnetic resonance imaging (MRI), magnetic resonance spectroscopy and neuropathological studies,³ and is in line with findings from ongoing studies using volumetric MRI in paediatric-onset patients (Sabatini, personal communication). Nevertheless, the disease pathophysiology of patients with HE HTT mutations, concurs with a more severe disease and worse prognosis.

To validate the findings from our study on brain tissues of patients with HE-PHD, we conducted an analysis of metabolic profiles in fibroblasts obtained from patients with HE-PHD. Our results revealed significantly reduced levels of GLUT-1 in both gene and protein expression, and a somewhat less pronounced decrease in GLUT-3 protein expression. However, no significant differences were observed in gene expression when compared to the healthy control. This discrepancy between findings in the brain tissues versus fibroblasts is likely explained by the fact that GLUT-3 is not the main transporter of glucose in peripheral cells such as fibroblasts.²⁹ While our data emphasize that the primary pathology in HE-PHD is found in the brain, they also highlight the probable existence of a peripheral component to the disease, as also suggested by our recent study which identified liver steatosis in patients with HE-PHD.⁵ The evidence of peripheral biological abnormalities may represent an important observation considering currently ongoing experimental therapies aimed at lowering mutated HTT in both the brain and periphery.³⁰

Since a direct relationship between GLUT function, neurodegeneration and neurodevelopment is still poorly understood, additional studies in HD and other neurodegenerative diseases are therefore needed due to its potential role in HD pathogenesis²⁰ and therapy perspectives.³¹ In fact, growing evidence suggests an important modulatory role for glucose transport in the HD mitochondrial deregulation, emphasizing that abnormal energy metabolism could interfere with brain neurodevelopment and may represent a critical therapeutic target for HD, as also suggested for adulthood disease.³² For instance, the GLUT-1 role in HE-PHD pathology suggests that a ketogenic diet could be beneficial for patients with HE-PHD when initiated in the early stages of the disease.¹¹ The high-fat ketogenic diet may result in permanent ketosis and provide the brain with an alternative energy

source. The beneficial effects of the ketogenic, normocaloric, with low carbohydrate intake diet, currently used in epilepsy and movement disorders, are well documented in children with GLUT-1 deficiency and may offer new therapeutic approaches to HE-PHD. This is especially important given that there is no validated experimental protocol so far to at least address any disease-modifying treatment against HE-PHD.

We are aware that our study has a number of limitations, the main one being that our HE-PHD brain donor cohort is limited to only two patients. This is due to the extremely rare occurrence of this variant. HD itself is a rare disease and only a small proportion of about 6% patients have juvenile-onset disease,¹⁴ and an even smaller proportion have HE-PHD. Thus, the opportunity to acquire a donor brain from a patient with HE-PHD is exceptionally rare. Likewise, owing to a general lack of donor brains from healthy controls, especially child donors, it was not possible to age-match our healthy control donor brain cohort to our HE-PHD cohort. It is therefore possible that some of the differences we observed between patients with HE-PHD and controls may have been due to differences in age rather than pathophysiology. Another limitation is due to the analysis of frontal cortex only, while an extensive study of several parts of brain and cortical regions might have offered additional insights. Unfortunately, we cannot provide a fine stratification of brain areas in our current context. This argues again that more cases and more extensive examination of the cerebral cortex are required to draw any firm conclusions.

An additional limitation is due to the clinical stratification of our adult cohort, specifically concerning the retrospective reconstruction of the approximate age of onset of JOHD. To limit such a bias, we included in the JOHD cohort only those patients with mutation size >55 CAG-repeats, a mutation size which is widely believed to be associated with JOHD.¹⁴ Notwithstanding these limitations, our findings shed light on the pathology of this devastating disease variant and highlight differences in potential biological mechanisms underlying HE-PHD and AOHD. Such differentiation may be important not only from a therapeutic perspective but also to ensure appropriate inclusion of paediatric patients into Huntington disease clinical trials.¹⁴

Finally, our study highlighted a difference in GLUT-1 expression between HE-PHD and JOHD. Such a biological difference, in addition to the CAG mutation length, suggests there may be a need to reconsider the old classification of HD variants and abandon the terminology “juvenile-onset”, which currently includes some adult-onset patients and instead replace this with the term “paediatric-onset” HD, to represent the category of patients that appears clinically and biologically different from adulthood HD.

REFERENCES

- MacDonald M.E., Ambrose C.M., Duyao M.P., et al. A novel gene containing a trinucleotide repeat that is expanded and unstable on Huntington's disease chromosomes. *Cell*. 1993;72(6):971–983. doi: 10.1016/0092-8674(93)90585-e.
- Tabrizi S.J., Langbehn D.R., Leavitt B.R., et al. Biological and clinical manifestations of Huntington's disease in the longitudinal TRACK-HD study: cross-sectional analysis of baseline data. *Lancet Neurol*. 2009;8(9):791–801. doi: 10.1016/S1474-4422(09)70170-X.
- Fusilli C., Migliore S., Mazza T., et al. Biological and clinical manifestations of juvenile Huntington's disease: a retrospective analysis. *Lancet Neurol*. 2018;17(11):986–993. doi: 10.1016/S1474-4422(18)30294-1.
- Cloud L.J., Rosenblatt A., Margolis R.L., et al. Seizures in juvenile Huntington's disease: frequency and characterization in a multicenter cohort. *Mov Disord*. 2012;27(14):1797–1800. doi: 10.1002/mds.25237.
- Squitieri F., Monti L., Graziola F., Colafati G.S., Sabatini U. Early liver steatosis in children with pediatric Huntington disease and highly expanded CAG mutations. *Park Relat Disord*. 2022;103:102–104. doi: 10.1016/j.parkreldis.2022.08.027.
- Tereshchenko A., Magnotta V., Epping E., et al. Brain structure in juvenile-onset Huntington disease. *Neurology*. 2019;92(17):e1939–e1947. doi: 10.1212/WNL.0000000000007355.
- Zhou X.Y., Lu J.Y., Zuo C.T., Wang J., Sun Y.M. juvenile-onset hypokinetic-rigid Huntington's disease: a case with dual-tracer positron emission tomography. *Quant Imaging Med Surg*. 2021;11(1):479–482. doi: 10.21037/qims-19-992.
- Gluchowska K., Pliszka M., Szablewski L. Expression of glucose transporters in human neurodegenerative diseases. *Biochem Biophys Res Commun*. 2021;540:8–15. doi: 10.1016/j.bbrc.2020.12.067.
- Benarroch E.E. Brain glucose transporters: implications for neurologic disease. *Neurology*. 2014;82(15):1374–1379. doi: 10.1212/WNL.0000000000000328.
- Seidner G., Alvarez M.G., Yeh J.I., et al. GLUT-1 deficiency syndrome caused by haploinsufficiency of the blood-brain barrier hexose carrier. *Nat Genet*. 1998;18(2):188–191. doi: 10.1038/ng0298-188.
- Leen W.G., Klepper J., Verbeek M.M., et al. Glucose transporter-1 deficiency syndrome: the expanding clinical and genetic spectrum of a treatable disorder. *Brain*. 2010;133(Pt 3):655–670. doi: 10.1093/brain/awp336.
- Ribaï P., Nguyen K., Hahn-Barma V., et al. Psychiatric and cognitive difficulties as indicators of juvenile huntington disease onset in 29 patients. *Arch Neurol*. 2007;64(6):813–819. doi: 10.1001/archneur.64.6.813.
- Nopoulos P.C., Aylward E.H., Ross C.A., et al. Smaller intracranial volume in prodromal Huntington's disease: evidence for abnormal neurodevelopment. *Brain*. 2011;134(1):137–142. doi: 10.1093/brain/awq280.
- Quarrell O.W.J., Nance M.A., Nopoulos P., et al. Defining pediatric huntington disease: time to abandon the term Juvenile Huntington disease? *Mov Disord*. 2019;34(4):584–585. doi: 10.1002/mds.27640.
- Zhang Y., Long J.D., Mills J.A., et al. Indexing disease progression at study entry with individuals at-risk for Huntington disease. *Am J Med Genet B Neuropsychiatr Genet*. 2011;156(7):751–763. doi: 10.1002/ajmg.b.31232.
- Di Domenico F., Tramutola A., Barone E., et al. Restoration of aberrant mTOR signaling by intranasal rapamycin reduces oxidative damage: focus on HNE-modified proteins in a mouse model of down syndrome. *Redox Biol*. 2019;23 doi: 10.1016/j.redox.2019.101162.

17. Klepinin A., Ounpuu L., Mado K., et al. The complexity of mitochondrial outer membrane permeability and VDAC regulation by associated proteins. *J Bioenerg Biomembr.* 2018;50(5):339–354. doi: 10.1007/s10863-018-9765-9.

18. Tramutola A., Lanzillotta C., Di Domenico F., et al. Brain insulin resistance triggers early onset Alzheimer disease in down syndrome. *Neurobiol Dis.* 2020;137. doi: 10.1016/j.nbd.2020.104772.

19. Ghosh C., Myers R., O'Connor C., et al. Cortical dysplasia in rats provokes neurovascular alterations, GLUT1 dysfunction, and metabolic disturbances that are sustained post-seizure induction. *Mol Neurobiol.* 2022;59(4):2389–2406. doi: 10.1007/s12035-021-02624-2.

20. Barnat M., Capizzi M., Aparicio E., et al. Huntington's disease alters human neurodevelopment. *Science.* 2020;369(6505):787–793. doi: 10.1126/science.aax3338.

21. Hickman R.A., Faust P.L., Rosenblum M.K., Marder K., Mehler M.F., Vonsattel J.P. Developmental malformations in Huntington disease: neuropathologic evidence of focal neuronal migration defects in a subset of adult brains. *Acta Neuropathol.* 2021;141(3):399–413. doi: 10.1007/s00401-021-02269-4.

22. De Vivo D.C., Trifiletti R.R., Jacobson R.I., Ronen G.M., Behmand R.A., Harik S.I. Defective glucose transport across the blood-brain barrier as a cause of persistent hypoglycorrachia, seizures, and developmental delay. *N Engl J Med.* 1991;325(10):703–709. doi: 10.1056/NEJM199109053251006.

23. Gamberino W.C., Brennan W.A. Glucose transporter isoform expression in Huntington's disease brain. *J Neurochem.* 1994;63(4):1392–1397. doi: 10.1046/j.1471-4159.1994.63041392.x.

24. McClory H., Williams D., Sapp E., et al. Glucose transporter 3 is a rab11-dependent trafficking cargo and its transport to the cell surface is reduced in neurons of CAG140 Huntington's disease mice. *Acta Neuropathol Commun.* 2014;2:179. doi: 10.1186/s40478-014-0178-7. BioMed Central Ltd.

25. Solis-Maldonado M., Mirò M.P., Acuña A.I., et al. Altered lactate metabolism in Huntington's disease is dependent on GLUT3 expression. *CNS Neurosci Ther.* 2018;24(4):343–352. doi: 10.1111/cns.12837.

26. Panov A.V., Gutekunst C.A., Leavitt B.R., et al. Early mitochondrial calcium defects in Huntington's disease are a direct effect of polyglutamines. *Nat Neurosci.* 2002;5(8):731–736. doi: 10.1038/nn884.

27. Han R., Liang J., Zhou B. Glucose metabolic dysfunction in neurodegenerative diseases—new mechanistic insights and the potential of hypoxia as a prospective therapy targeting metabolic reprogramming. *Int J Mol Sci.* 2021;22(11):5887. doi: 10.3390/ijms22115887.

28. Mergenthaler P., Kahl A., Kamitz A., et al. Mitochondrial hexokinase II (HKII) and phosphoprotein enriched in astrocytes (PEA15) form a molecular switch governing cellular fate depending on the metabolic state. *Proc Natl Acad Sci U S A.* 2012;109(5):1518–1523. doi: 10.1073/pnas.1108225109.

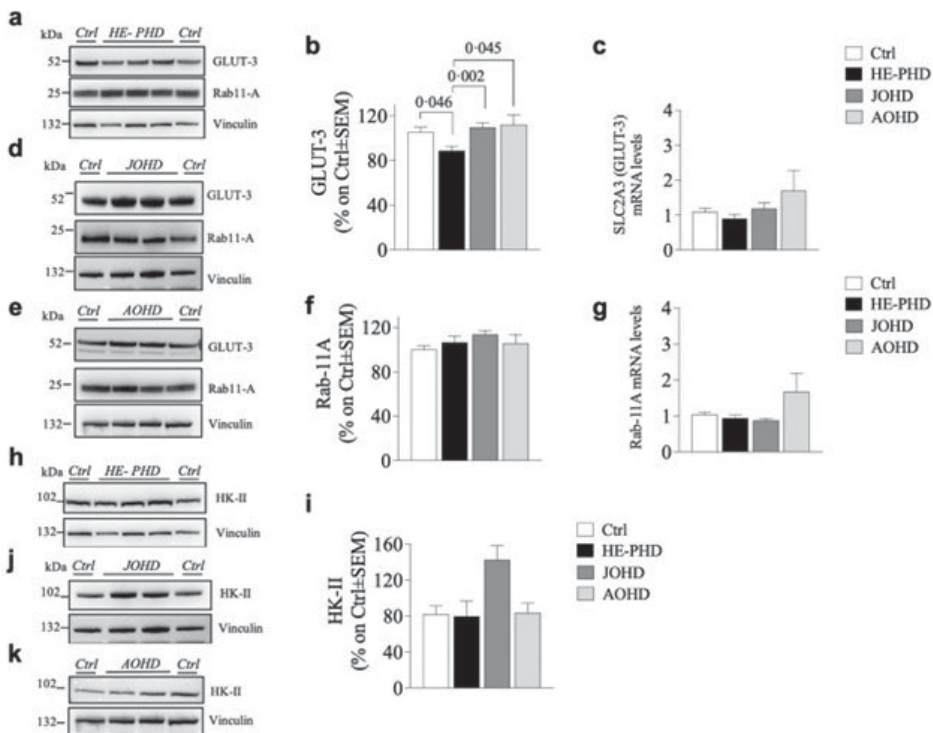
29. Simpson I.A., Dwyer D., Malide D., Moley K.H., Travis A., Vannucci S.J. The facilitative glucose transporter GLUT3: 20 years of distinction. *Am J Physiol Metab.* 2008;295(2):E242–E253. doi: 10.1152/ajpendo.90388.2008.

30. Bhattacharyya A., Trotta C.R., Narasimhan J., et al. Small molecule splicing modifiers with systemic HTT-lowering activity. *Nat Commun.* 2021;12(1):1–12. doi: 10.1038/s41467-021-27157-z. 2021 121.

31. Braz B.Y., Wennagel D., Ratiñ L., et al. Treating early postnatal circuit defect delays Huntington's disease onset and pathology in mice. *Science.* 2022;377(6613). doi: 10.1126/science. abq5011.

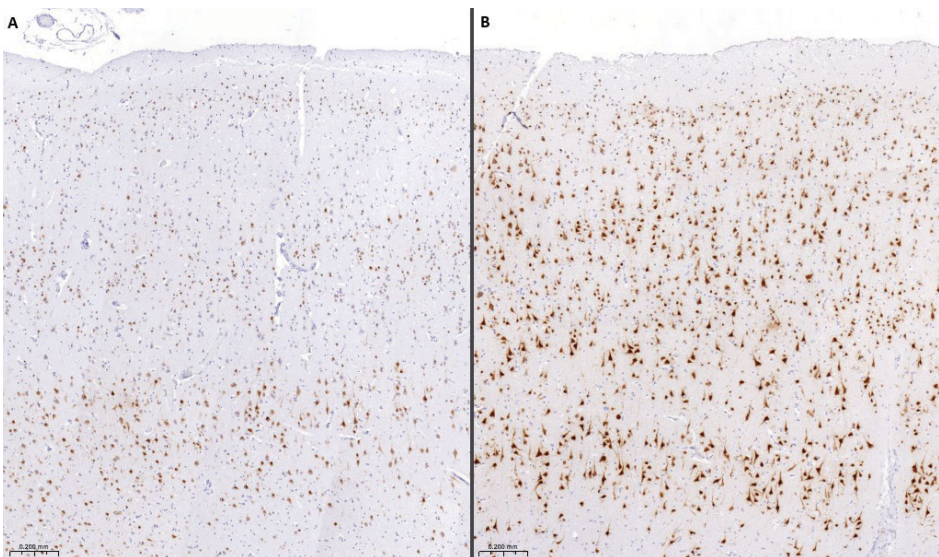
32. Saft C., Zange J., Andrich J., et al. Mitochondrial impairment in patients and asymptomatic mutation carriers of Huntington's disease. *Mov Disord.* 2005;20(6):674–679. doi: 10.1002/mds.20373.

SUPPLEMENTARY FIGURES



Supplementary Figure S1. Evaluation of GLUT-3, Rab11-A and HK-II levels in fibroblasts of HE-PHD, JOHD, AOHD patients and controls.

Representative western blot images and densitometric evaluation of GLUT-3, Rab11-A (a, b, d, e, f-g) and HK-II (h-k) protein levels normalized to Vinculin protein levels in fibroblasts of HE-PHD, JOHD, AOHD patients and age-matched controls. All densitometric values are reported as a percentage of controls (set at 100%) and are the mean \pm SEM of three independent experiments. ($p<0.05$, one-way ANOVA with Tukey post-hoc test). qRT-PCR analysis of GLUT-3 and Rab11-A total mRNA in fibroblasts of HE-PHD, JOHD, AOHD patients and age-matched controls (c, g). Relative mRNA expression levels are reported as a percentage of GAPDH expression levels (set at 100%) and are the mean \pm SEM of three experiments ($p<0.05$, with Tukey post-hoc test). The use of the same loading control in different figures serves as a representative image. Each individual protein has been normalized against its respective loading control.



Supplementary Figure S2. NeuN staining in the frontal cortex of HE-PHD patients

IHC staining of NeuN in the FrCx of HE-PHD HD86 (a) and HD252 (b) donors.